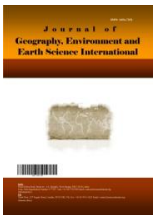

Journal of Geography, Environment and Earth Science International

23(3): 1-19, 2019; Article no.JGEESI.51594
ISSN: 2454-7352

Petrology and Geochemistry of Hama Koussou Dolerite Dyke Swarms (North Cameroon, Central Africa)

Fagny Mefire Aminatou[1], Bardintzeff Jacques-Marie[2*], Nkouandou Oumarou Faarouk[1], Lika Gbeleng Thomas d'Aquin[1] and Ngougoure Mouansie Samira[1]

[1]Faculty of Science, University of Ngaoundéré, P.O.Box. 454, Ngaoundéré, Cameroon.
[2]Sciences de la Terre, Volcanologie, Université Paris-Sud, UMR CNRS 8148 GEOPS, Bât 504, Université Paris-Saclay, F-91405 Orsay, France.

Authors' contributions

This work was carried out in collaboration among all authors. Authors FMA, NOF, LGTA and NMS made field work. Author NOF designed the study and the selections of samples for analyses and wrote the protocol. Author BJM made analyses of minerals phases with microprobe. Author FMA wrote the first draft of the manuscript and managed the literature. Author NOF improved the manuscript. Author BJM wrote the final version of the manuscript. All authors read and approved the final manuscript.

Article Information

DOI: 10.9734/JGEESI/2019/v23i330170
Editor(s):
(1) Dr. Onuigbo Evangeline Njideka, Senior Lecturer, Department of Geological Sciences, Faculty of Physical Sciences, Nnamdi Azikiwe University, Nigeria.
Reviewers:
(1) J Dario Aristizabal-Ochoa, Universidad Nacional de Colombia, Colombia.
(2) J. Marvin Herndon, USA.
(3) Breno Barra, Federal University of Santa Catarina (UFSC), Brazil.
Complete Peer review History: http://www.sdiarticle4.com/review-history/51594

Original Research Article

Received 06 July 2019
Accepted 16 September 2019
Published 03 October 2019

ABSTRACT

The Pan African granitoid basement of Hama Koussou Cretaceous half basin in North Cameroun (Central Africa) is transected by near N-S, NE-SW and ENE-WSW giant doleritic dykes trending along the same Pan African directions. Hama Koussou dolerites are compliant with the regional distension that occurred after the Pan African basement consolidation prior to the development of West and Central African Rift System at Late Jurassic-Early Cretaceous times. Studied lavas are composed of large clinopyroxene oïkocrysts, plagioclase and alkali feldspar laths and oxides phenocrysts exhibiting ophitic, sub-ophitic and intercertal textures. Microprobe chemical analyses

**Corresponding author: E-mail: jacques-marie.bardintzeff@u-psud.fr;*

carry out on the main mineral phases show that clinopyroxenes are diopside and augite, plagioclases are labradorite, andesine, oligoclase and albite and alkali feldspars are mainly sanidine with a few percent of orthoclase. ICP-MS and ICP-AES geochemical analyses of Hama Koussou lavas exhibit basalt, basaltic trachyandesite and trachyandesite compositions of continental tholeiite features. Tholeiite basalts of Hama Koussou are the results of high partial melting of E-MORB mantle source of spinel lherzolite composition, located at 65-55 km depth. More evolved tholeiite lavas of Hama Koussou basin are the products of tholeiite basalt differentiation trough assimilation and fractional crystallization coupled with fluids circulation.

Keywords: Dolerite; dyke swarm; continental tholeiite; Pan African; Hama Koussou; Cameroon, Central Africa.

1. INTRODUCTION

The Hama Koussou Cretaceous half basin belongs to the group of Barremo-Aptian intra-continental basins of Northern Cameroon formed within the Pan African granito-gneissic basement Fig. 1, [1]. This basin is filled by 1000 to 3000 m thick sedimentary pile comprising basal sandstones, microconglomerate levels of about 10 m in thickness, thick shaly sequence with intercalated layers of siltstones, carbonate siltstones and dolomites [1]. Numerous lava flows of alkali basalt composition and doleritic dykes cut across the series of the whole basin. The Barremo-Aptian intracontinental basins of Northern Cameroon are small is shape compared to the large Albo-Aptian basins of Benue trough in Nigeria which propagates both into Northern Cameroon via its Yola branch into Southern Chad Republic [1,2,3]. The first group of small basins of Northern Cameroon are supposed to be initiated from the opening of central part of Atlantic ocean while those of surrounding area have been formed through the opening of the Gulf of Guinea, respectively at Barremian (126 My) and Albian (110 My) times [4]. This leads to at least two fracturing episodes that have affected this part of Africa during the Lower Cretaceous [1]. Major studies carry out on the Northern Cameroon basins have used to decipher the hydrocarbon index trough the structural and sedimentary petrology [3]. The relations between the fracturing episodes and dolerite dykes of the Barremo-Aptian intra-continental basins of the Northern Cameroon are poorly known. As time markers, the geodynamic implications of dolerites dykes of those basins are not yet elucidated and their petrologic data still lacking particularly those of Hama Koussou dolerites.

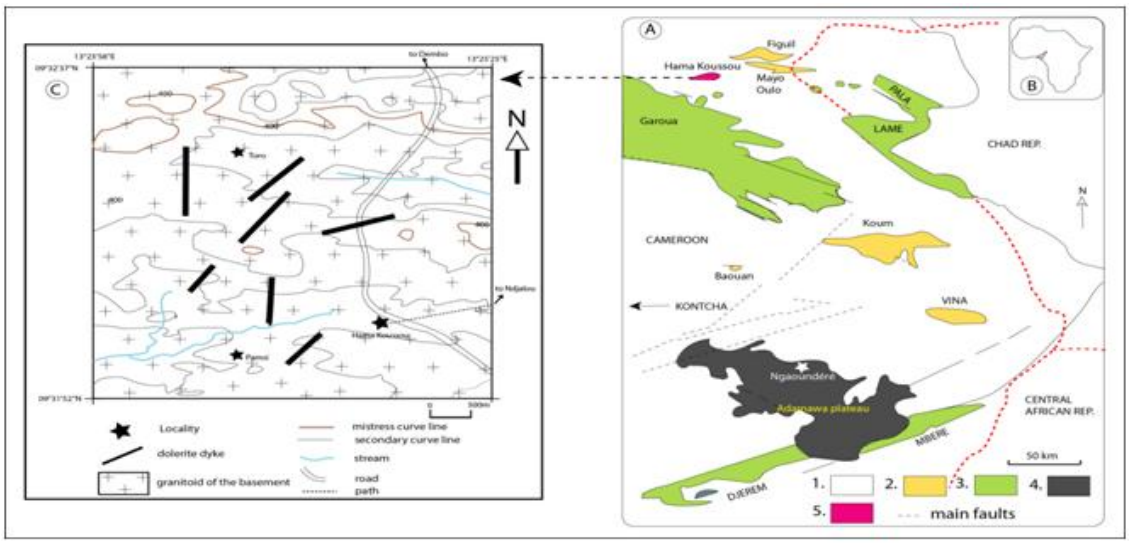

Fig. 1. A: Location of Baremo-Aptian up to Turonian sedimentary basins of the Northern Cameroon (modified and redrawn after [1]) in Africa (B). 1. PanAfrican basement; 2. Baremo-Aptian basin; 3. Albo-Aptian to Cenomano-Turonian basin; 4. Mio-Pliocene volcanism of Adamawa Plateau [10]; 5. Hama Koussou basin (this study). C: Sketch map of Hama Koussou Cretaceous basin

The main goal of this work is to examine the petrology and geochemistry features of dolerite dykes from the Hama Koussou Cretaceous basin in the Central North Cameroon, to determine their petrogenetic processes and help sort out their geodynamic implications.

2. GEOLOGICAL SETTING

The Northern Cameroon basins (see Fig. 1) belong to the Central African Rift System basins developed at the Late Jurassic-Early Cretaceous time [5], from weak crust of the Northern part of Central Africa Fold Belt Chain (CAFBC, [6,7]. The Northern Cameroonian basins are presented [1] as asymmetrical synclines along the E-W axis. Those authors have suggested that the asymmetry of the structure is mainly due to major faults which are particularly expressed on one side of the basins which subsidence was governed by a regime of approximately N-S-trending crustal extension [8]. More recent studies have shown that the sedimentation rates of Hama Koussou deposits varied between 5.5 cm/kyr and 40.88 cm/kyr [9], leading to the filling of the basin by an alternation of fine grained sandstone, siltstone and mudstone, coarse sandstone, micro-conglomerate and conglomerate facies at the base. The same materials are found in the Baouan basin at the South [1]. The directions of magnetization reveal three polarities in the Hama Koussou basin, suggesting an age between 128-125 My [9]. The similar studies are not yet done in some Northern Cameroonian basins. Volcanic products are restricted to limited lava flows of transitional and alkali series associated to dolerite dykes [1].

3. MATERIALS AND METHODS

Petrography studies were carried out on 15 thin sections prepared from the representative samples of the dyke swarms at the laboratory GEOPS of the Faculty of Science, University of Paris-Sud Orsay, France. All thin sections have undergone the preliminary phase of metallization before the electron microprobe SX 100 analyses in the Service Camparis of the University of Paris Sorbonne, France. The operating conditions were an accelerating voltage and a beam current as follows: Clinopyroxene: 15 kV and 40 nA, 20 s except Ti for clinopyroxene (30 s); plagioclase, K-feldspar: 10 s; titanomagnetite: Si, Ca, Ni: 10 s; Mn: 25 s; Cr; 15 s; Al: 30 s; Ti, Fe, Mg: 40 s. Standards used were a combination of natural and synthetic minerals. Data corrections were made using a PAP method correction of [11] Pouchou and Pichoir (1991). Major and trace element analyses of lavas were determined through 5 representative samples by ICP-AES and ICP-MS at the Acmel laboratory of Vancouver, Canada. A single sample was analyzed at the “Centre de Recherche Pétrographique et Géochimique, CRPG” of Nancy, France. The prepared sample was mixed with $LiBO_2/Li_2B_4O$ flux. Crucibles are fused in a furnace. The cooled bead was dissolved in ACS grade nitric acid and analyzed by ICP and/or ICP-MS. Loss on ignition (LOI) was determined by igniting a sample split then measuring the weight loss.

4. RESULTS

4.1 Field Work and Petrography

Studied dykes swarms are 7 to 12 meters thick (Table 1) and show N05 and N50 to N70 trending directions (Fig. 2A) different from the lineaments of the basement (Fig. 2B). Dolerite dykes from Hama Koussou half basin crosscut vertically to sub-vertically the metamorphic gneiss of the basement (Figs. 3A and 3C). They are composed of blocks and bowls of 20 cm to 1.2 m wide showing chaotic disposition. Greyish and greenish matrix of representative samples (Figs. 3B and 3D) are covered by thin (1 to 2 cm) greenish white patina. Majority of outcrops exhibits the coarse granular structure showing a few percent whitish feldspar megacrysts 0.5 to 1.5 cm in size. Matrix contain 5 to 10 volume percent of feldspar phenocrysts, yellowish squared crystals of pyrite (1 to 2 mm and 1 to 3 volume %) and rare dark crystals of pyroxene? amphibole? or oxides (3 to 5 volume %). Fine acicular (1 to 2 mm) microlites of feldspar crystals are also present.

Studied dolerite samples with microscope exhibit intercertal (Fig. 4A), sub-ophitic (Figs. 4B and 4C) to ophitic (Fig. 4D) textures. They are composed of abundant (more than 20 volume %) euhedral crystals of sieved and skeletal plagioclase and alkali feldspar showing light thin corona of 0.2 to 0.4 mm, skeletal oxides and green patches of altered clinopyroxene crystals. Chlorite crystals of greenish color are present. Samples with ophitic and sub-ophitic textures show large crystals of yellowish clinopyroxene oikocrysts (Fig. 4D). Some clinopyroxene and feldspar crystals contain inclusion of oxides microcrysts.

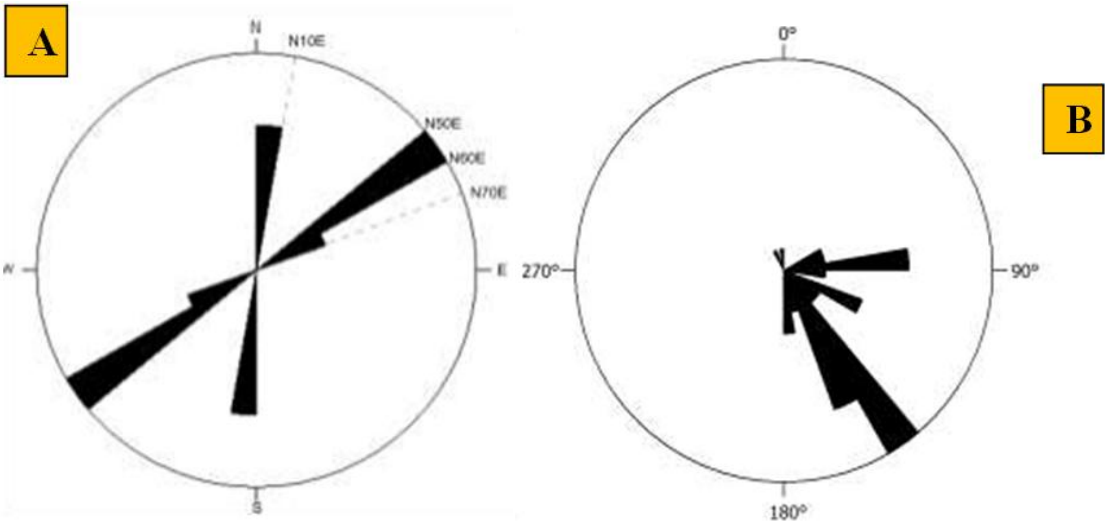

Fig. 2. A: Trending directions of dolerite dykes of Hama Koussou half basin and B: Main orientation trends of crustal discontinuities

Table 1. Main characteristic features of some dolerite dykes of Hama Koussou Cretaceous basin

Number	Sample	Location	Direction	Width (m)
1	HB2	09°32'15.55'' 13°24'31''	N50E	8-10
2	L1	09°32'15.59'' 13°24'30.8''	N70E	10-11
3	HB3	09°32'14.6'' 13°24'31''	N52E	12
4	M5	09°32'11.4'' 13°24'30''	N55E	11-12
5	J4	09°32'14'' 13°24'30.5''	N05E	9
6	J6	09°32'10.8'' 13°24'30.4''	N06E	7

4.2 Mineralogy

Microprobe chemical analyses of some mineral phases of dolerite dyke from Hama Koussou are presented in Tables 2 to 4. Clinopyroxene, plagioclase and alkali feldspar have been analyzed.

The results of clinopyroxene analyses are presented in Table 2 and plotted in the pyroxene quadrilateral diagram (Fig. 5, after [12]). Analyzed clinopyroxenes are diopsides (Wo_{45-47} En_{45-50} Fs_{3-9}) and essentially augites (Wo_{35-45} En_{39-50} Fs_{6-21}). They exhibit rather high Al_2O_3 contents (up to 6.7 wt. %) and low TiO_2 contents (0.2-0.8 wt. %). There are a continuous decrease in Ca and an increase in Fe2+ contents from diopside to augite (Fig. 5). Si (apfu) contents are always under 2 cations in structural formulae. Relatively low Mg# (Mg# = Mg/(Mg+Fe)) number are bracketed between 0.67 and 0.84.

The plagioclase chemical compositions (Table 3 and Fig. 6B) evolved toward a decrease in Ca content from labradorite (only in basalt) (An53.2-59.3) to albite type (An2.8-7.3) via andesine (An37.8-39.2) and oligoclase (An10.9-29.6). FeO contents are always low (< 1 wt. %).

The alkali feldspar compositions (Table 4 and Fig. 6A) is dominantly sanidine (Or39.7-95.6 and Ab4.3-57.7) with small amount of anorthoclase (Or14.7-32.5 and Ab64.3-81.5). BaO (up to 0.7 wt. %) and FeO (up to 1.0 wt. %) contents are relatively high. Note that alkali feldspars are absent in basalt and anorthoclase does exist only in basaltic trachyandesite.

Fig. 3. A: Greyish dolerite dyke (J4) and B: representative sample (L1) showing coarse granular structure and white feldspar phenocrysts. C: Greenish dolerite dyke (M5) and D: representative sample (J6) containing feldspar phenocrysts. Coin diameter = 3 cm

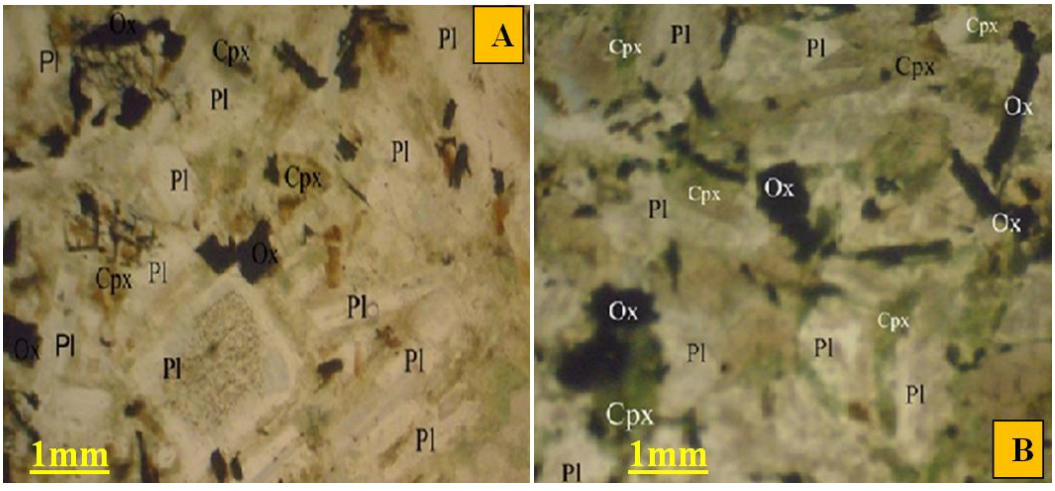

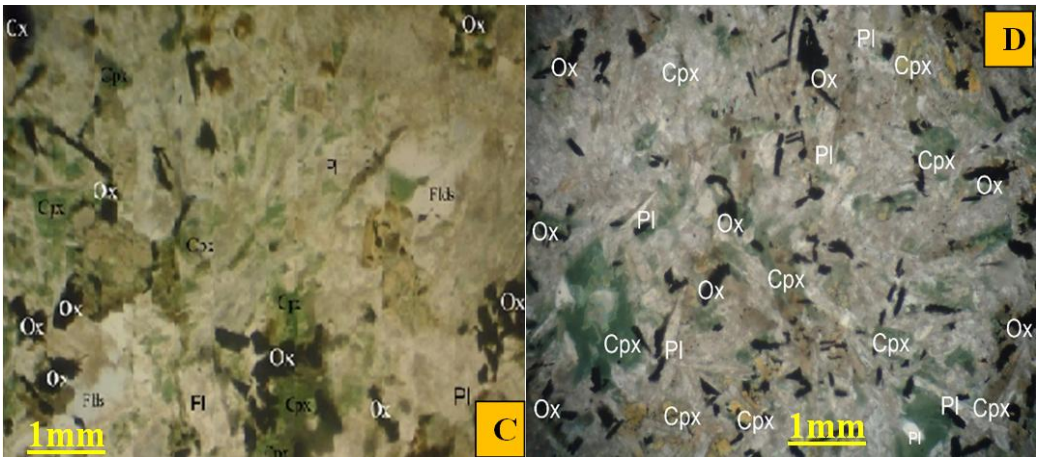

Fig. 4. Microscopic view of main textures (intersertal: A, sub-ophitic: B and C and ophitic: D) of Hama Koussou dolerites (seen in LPNA). Cpx = clinopyroxene, Pl = plagioclase, Ox = Fe-Ti oxide

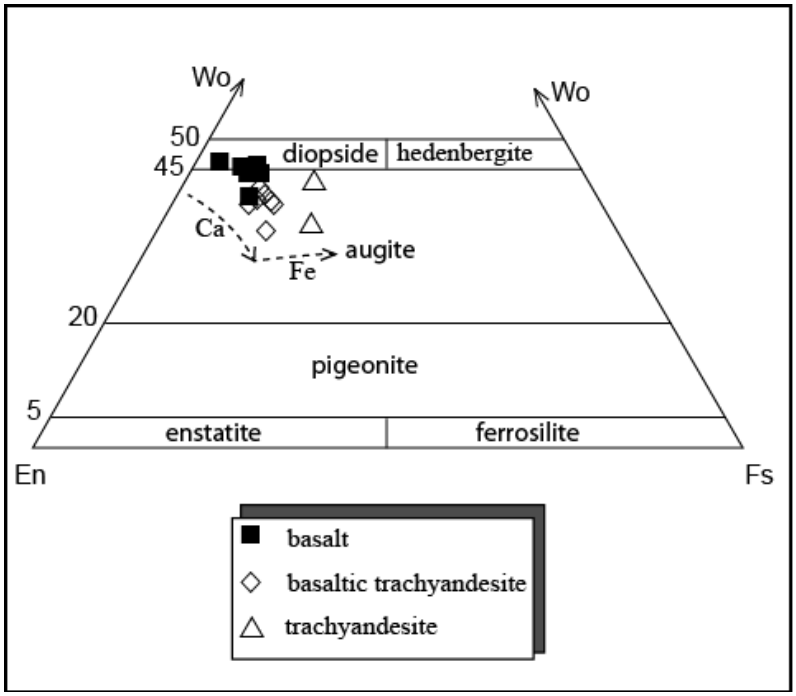

Fig. 5. Clinopyroxene compositions of Hama Koussou dolerites in Wo-En-Fs diagram after the classification scheme of [12]

4.3 Geochemical Features

ICP-MS and ICP-AES chemical analyses of dolerite dykes of the Hama Koussou half basin (Table 5) exhibit basalt, basaltic trachyandesite and trachyandesite compositions (Fig. 7) following [13]. SiO_2 contents (46.5 to 56 wt. %) are within the range of some dolerites worldwide (Karoo: 50.6 to 53.6 wt. %, Tasmanian: 53.8 wt. %, Antarctic Ferrar: 53 wt. %) compositions [14]. Relatively low TiO_2 contents of the Hama Koussou dolerites (1.7 to 3 wt. %) are typical of low TiO_2 continental tholeiites. MgO contents decreased from basalt to trachyandesite (5.6 to 3.2 wt. %) while FeO contents strongly decrease (13.8 to 7.4 wt. %) leading to contrasting Mg# values (=100*(MgO/40.32)/((MgO/40.32)+(FeOt/71.85)). Mg# of doleritic basalt are relatively

constant (47.0-47.9), lower (42) in basaltic trachyandesite and higher (48.8 to 49.9) in trachyandesite. Alkali contents are relatively high and increase from basalt (4.5 wt. %) to tranchyandesite (7.5 wt. %). The Hama Koussou dolerites of basaltic composition are saturated lavas (lack of both nepheline and quartz normative composition) while basaltic trachyandesite and trachyandesite are quartz normative (2.1-3.9 wt. %). Hama Koussou dolerites plot in continental tholeiite field defined in the TiO_2-K_2O-P_2O_5 diagram (Fig. 8A).

Contents of transitional elements Ni, Cr and Co are low (14-44, 1.2-6.7 and 21-49 ppm, respectively). Rb contents decrease from basalt (110 ppm) to evolved lavas (lowest contents of Rb - 24.5 ppm - are found in basaltic trachyandesite). Sr and Ba contents are high and increase from basalt (608 and 443 ppm) to trachyandesite (855 and 1419 ppm). Zr and Th contents increase from basalt to trachyandesite whereas Y, Nb and Ta decrease. Zr/Hf ratios (42-44) are relatively constants. Values of Zr/Nb ratios are between 11 and 24 and Zr/Y between 8 and 20 increasing from basalt to evolved dolerites. Nb/Ta ratios (15.8-17.5 in basalt, 12.6 in one basaltic trachyandesite and 14.8-16.3 for trachyandesite) show contrast variations. Y/Nb ratios are higher than 1 (1.2 to 1.3). Th/Ta ratios of studied dolerites distinguish two groups with first group showing Th/Ta close to 1 in more basaltic dolerites and close to 14-15 in the second group of evolved lavas. In Th-3xTb-2xTa triangle (Fig. 8B) of [16], trachyandesite dolerites fall in the orogenic field whereas basalt and basaltic trachyandesite dolerites fall within the intermediate domain of continental tholeiites. In Y/15-La/10-Nb/8 triangle diagram (Fig. 8C) of [17], trachyandesite dolerites fall in the compressive orogenic domain when basalt and basaltic trachyandesite dolerites are within the intracontinental post orogenic domain.

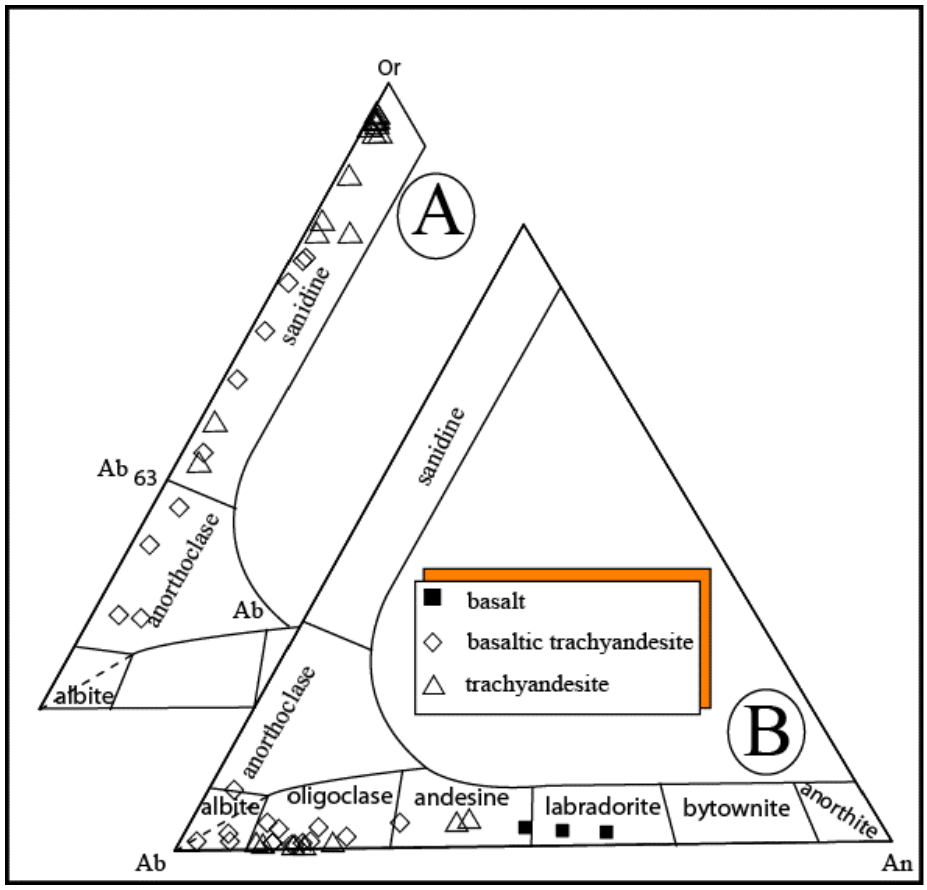

Fig. 6. Composition of (A) alkali feldspar and (B) plagioclase of Hama Koussou dolerites in Or-Ab-An diagrams

Table 2. Clinopyroxene microprobe analyses of Hama Koussou dolerites

Sample	HB2										HD3						
SiO_2 (wt.%)	51.90	50.25	51.24	49.84	49.58	50.08	50.39	47.78	50.94	47.66	47.53	53.34	45.97	49.31	56.05	45.06	48.49
TiO_2	0.41	0.28	0.41	0.61	0.70	0.61	0.31	0.61	0.26	0.84	0.72	0.15	0.74	0.46	0.45	0.74	0.38
Al_2O_3	2.95	4.80	3.87	4.25	4.07	3.76	2.90	5.37	2.84	5.74	5.20	5.63	6.69	4.76	4.61	6.64	4.15
Cr_2O_3	0.00	0.00	0.01	0.01	0.00	0.02	0.02	0.05	0.01	0.01	0.00	0.00	0.00	0.01	0.00	0.03	0.00
FeO	10.12	10.38	9.55	10.40	9.85	9.64	10.49	10.47	10.13	10.83	10.45	10.40	11.22	10.26	9.27	11.37	10.29
MnO	0.31	0.41	0.35	0.31	0.26	0.34	0.40	0.18	0.20	0.25	0.22	0.32	0.20	0.21	0.13	0.23	0.25
MgO	14.93	14.91	14.45	13.93	14.46	14.10	15.03	12.47	15.13	12.67	12.61	11.81	11.81	12.88	11.14	11.75	13.20
CaO	19.87	18.26	20.68	19.86	19.98	20.90	19.56	21.46	20.51	21.66	21.79	16.11	21.39	22.26	19.62	21.70	21.79
Na_2O	0.37	0.34	0.43	0.40	0.36	0.38	0.37	0.46	0.31	0.48	0.48	1.48	0.44	0.52	0.32	0.55	0.49
sum	100.87	99.62	100.97	99.61	99.26	99.82	99.48	98.84	100.32	100.14	99.01	99.25	98.47	100.67	101.58	98.08	99.04
Si (a.p.f.u.)	1.910	1.868	1.882	1.861	1.853	1.864	1.879	1.803	1.882	1.776	1.790	1.998	1.745	1.825	2.077	1.716	1.822
Ti	0.011	0.008	0.011	0.017	0.020	0.017	0.009	0.017	0.007	0.024	0.020	0.004	0.021	0.013	0.013	0.021	0.011
Al	0.128	0.210	0.167	0.187	0.179	0.165	0.127	0.239	0.124	0.252	0.231	0.249	0.299	0.208	0.202	0.298	0.184
Cr	0.000	0.000	0.000	0.000	0.000	0.001	0.000	0.001	0.000	0.000	0.000	0.000	0.000	0.000	0.000	0.001	0.000
Fe+++	0.055	0.062	0.077	0.084	0.101	0.100	0.123	0.153	0.120	0.183	0.183	0.000	0.200	0.154	0.000	0.267	0.187
Fe++	0.257	0.261	0.216	0.240	0.207	0.199	0.204	0.178	0.193	0.154	0.146	0.326	0.156	0.164	0.287	0.096	0.136
Mn	0.010	0.013	0.011	0.010	0.008	0.011	0.013	0.006	0.006	0.008	0.007	0.010	0.007	0.007	0.004	0.007	0.008
Mg	0.819	0.826	0.791	0.776	0.806	0.782	0.836	0.701	0.833	0.704	0.708	0.659	0.669	0.711	0.615	0.667	0.740
Ca	0.783	0.727	0.814	0.795	0.800	0.833	0.782	0.868	0.812	0.865	0.879	0.647	0.870	0.882	0.779	0.886	0.877
Na	0.026	0.024	0.031	0.029	0.026	0.028	0.027	0.034	0.022	0.035	0.035	0.107	0.033	0.037	0.023	0.041	0.036
Wo	39.42	35.41	41.13	39.83	40.08	42.21	39.27	44.58	40.97	44.44	45.53	36.48	44.61	45.78	43.17	46.60	45.57
En	46.44	49.52	46.76	46.56	48.58	46.92	49.97	45.77	49.11	47.63	47.21	42.51	47.32	45.59	38.74	50.44	48.04
Fs	14.14	15.08	12.11	13.60	11.34	10.87	10.75	9.65	9.93	7.93	7.26	21.01	8.07	8.62	18.09	2.96	6.39

Table 3. Plagioclase microprobe analyses of the Hama Koussou dolerites

Sample	HB2														
SiO_2 (wt. %)	56.43	66.33	59.61	64.53	65.17	64.40	61.85	60.80	65.80	56.48	65.18	63.57	54.46	65.39	61.23
Al_2O_3	26.42	20.91	25.03	22.48	21.29	22.28	23.57	24.99	21.80	26.47	22.68	23.98	27.87	22.11	24.29
FeOt	0.69	0.21	0.71	0.13	0.13	0.16	0.50	0.39	0.17	0.71	0.09	0.49	0.93	0.08	0.45
CaO	9.90	1.42	8.08	3.87	2.63	4.06	6.19	4.64	2.89	9.89	2.86	2.43	11.16	3.52	3.71
Na_2O	5.66	10.99	6.90	9.97	10.51	9.68	7.62	8.22	10.28	5.64	10.05	8.49	5.11	9.73	8.66
K_2O	0.62	0.45	0.73	0.16	0.14	0.19	0.75	0.32	0.16	0.63	0.14	0.48	0.48	0.12	0.56
BaO	0.00	0.04	0.10	0.09	0.03	0.05	0.14	0.00	0.02	0.11	0.03	0.00	0.00	0.00	0.31
sum	99.72	100.35	101.16	101.23	99.90	100.82	100.62	99.36	101.12	99.94	101.04	99.44	100.00	100.96	99.20
Si (a.p.f.u.)	2.552	2.910	2.646	2.822	2.876	2.826	2.740	2.711	2.868	2.551	2.842	2.805	2.467	2.855	2.739
Al	1.408	1.081	1.310	1.159	1.107	1.153	1.231	1.313	1.120	1.409	1.165	1.247	1.488	1.138	1.281
Fe3+	0.026	0.008	0.026	0.005	0.005	0.006	0.019	0.014	0.006	0.027	0.003	0.018	0.035	0.003	0.017
Ca	0.480	0.067	0.385	0.181	0.125	0.191	0.294	0.222	0.135	0.478	0.134	0.115	0.542	0.165	0.178
Na	0.496	0.935	0.594	0.846	0.900	0.824	0.655	0.711	0.869	0.494	0.850	0.727	0.449	0.824	0.751
K	0.036	0.025	0.041	0.009	0.008	0.010	0.042	0.018	0.009	0.037	0.008	0.027	0.028	0.007	0.032
Ba	0.000	0.001	0.002	0.002	0.000	0.001	0.002	0.000	0.000	0.002	0.000	0.000	0.000	0.000	0.005
Or	3.55	2.48	4.05	0.85	0.78	1.02	4.27	1.93	0.90	3.62	0.80	3.11	2.71	0.70	3.31
Ab	49.05	91.04	58.23	81.66	87.16	80.36	66.10	74.77	85.80	48.96	85.72	83.68	44.12	82.77	78.20
An	47.40	6.48	37.72	17.49	12.06	18.63	29.63	23.30	13.30	47.42	13.48	13.21	53.17	16.53	18.50

Table 3 (continued)

Sample	HB2												
SiO_2 (wt. %)	57.58	54.03	65.21	64.55	63.64	68.61	65.38	64.65	64.00	65.24	64.63	64.75	65.84
Al_2O_3	25.13	28.38	22.28	22.58	23.16	19.67	20.69	21.66	22.50	21.93	22.25	21.88	20.29
FeOt	0.94	0.59	0.07	0.24	0.28	0.23	0.23	0.26	0.03	0.05	0.28	0.08	0.32
CaO	8.31	12.31	3.43	3.85	4.83	0.60	2.42	2.30	3.73	3.23	3.58	3.57	1.59
Na_2O	6.60	4.38	9.74	9.64	9.54	11.37	10.17	10.25	9.67	10.15	9.97	10.05	11.08
K_2O	0.82	0.44	0.12	0.10	0.19	0.19	0.78	0.22	0.07	0.08	0.08	0.10	0.19
BaO	0.05	0.03	0.14	0.00	0.09	0.00	0.08	0.05	0.03	0.06	0.00	0.01	0.03
sum	99.43	100.15	100.99	100.95	101.63	100.66	99.76	99.39	100.04	100.73	100.79	100.45	99.32
Si (a.p.f.u.)	2.608	2.446	2.848	2.824	2.780	2.982	2.896	2.866	2.825	2.857	2.833	2.847	2.918
Al	1.342	1.514	1.147	1.164	1.192	1.008	1.080	1.131	1.170	1.132	1.149	1.134	1.060

Sample							HB2						
Fe3+	0.036	0.022	0.003	0.009	0.010	0.008	0.009	0.010	0.001	0.002	0.010	0.003	0.012
Ca	0.403	0.597	0.160	0.180	0.226	0.028	0.115	0.109	0.176	0.152	0.168	0.168	0.075
Na	0.580	0.385	0.825	0.818	0.808	0.959	0.873	0.882	0.828	0.862	0.848	0.857	0.952
K	0.047	0.025	0.007	0.005	0.010	0.010	0.044	0.012	0.004	0.004	0.004	0.006	0.011
Ba	0.001	0.000	0.002	0.000	0.002	0.000	0.001	0.001	0.000	0.001	0.000	0.000	0.000
Or	4.59	2.50	0.68	0.54	1.00	1.03	4.25	1.21	0.38	0.42	0.43	0.54	1.03
Ab	56.26	38.22	83.15	81.50	77.35	96.18	84.63	87.88	82.12	84.69	83.08	83.16	91.72
An	39.15	59.28	16.17	17.97	21.65	2.79	11.12	10.91	17.50	14.89	16.48	16.30	7.25

Table 4. Alkali feldspar microprobe analyses of the Hama Koussou dolerites

Sample							HB2							
SiO_2 (wt. %)	73.31	64.64	64.60	84.76	64.75	65.03	66.75	65.36	66.41	66.58	70.57	65.23	67.58	65.21
Al_2O_3	15.18	18.27	18.50	8.28	17.95	18.06	19.33	18.37	18.51	18.90	16.73	21.17	19.26	18.28
FeOt	0.14	0.41	0.15	0.11	0.41	0.31	0.10	0.59	0.26	0.36	0.31	0.56	0.20	0.24
CaO	0.06	0.04	0.25	0.00	1.18	0.03	1.46	0.30	0.19	0.33	0.51	0.72	0.27	0.06
Na_2O	0.35	0.69	0.70	0.22	2.04	0.61	9.45	2.99	3.43	5.31	6.04	9.33	5.93	0.58
K_2O	12.03	15.70	15.45	7.30	13.15	16.10	2.70	12.50	11.72	9.38	6.32	2.62	8.05	16.25
BaO	0.21	0.18	0.57	0.05	0.08	0.28	0.00	0.22	0.48	0.34	0.27	0.09	0.09	0.22
sum	101.28	99.94	100.22	100.71	99.55	100.42	99.79	100.33	101.00	101.20	100.77	99.72	101.38	100.84
Si (a.p.f.u.)	3.410	2.992	2.989	4.061	2.989	2.997	2.955	2.980	3.005	2.973	3.177	2.878	3.002	2.992
Al	0.832	0.997	1.009	0.467	0.976	0.981	1.008	0.987	0.987	0.995	0.888	1.101	1.009	0.989
Fe	0.006	0.016	0.006	0.004	0.016	0.012	0.004	0.022	0.010	0.013	0.012	0.021	0.007	0.009
Ca	0.003	0.002	0.013	0.000	0.058	0.001	0.069	0.015	0.009	0.016	0.025	0.034	0.013	0.003
Na	0.032	0.062	0.063	0.020	0.182	0.055	0.812	0.265	0.301	0.460	0.528	0.798	0.511	0.052
K	0.714	0.927	0.912	0.446	0.774	0.947	0.152	0.727	0.676	0.535	0.363	0.148	0.456	0.951
Ba	0.004	0.003	0.010	0.001	0.001	0.005	0.000	0.004	0.008	0.006	0.005	0.002	0.002	0.004
Or	95.36	93.50	92.37	95.57	76.28	94.40	14.74	72.23	68.57	52.91	39.67	15.07	46.55	94.58
Ab	4.26	6.28	6.36	4.38	17.98	5.48	78.54	26.30	30.48	45.55	57.65	81.46	52.12	5.14
An	0.38	0.22	1.27	0.05	5.74	0.13	6.71	1.47	0.96	1.54	2.68	3.48	1.33	0.28

Table 4 (continued)

Sample	HB2													
SiO_2 (wt. %)	65.81	66.31	65.12	65.29	64.33	64.90	66.15	65.16	66.28	65.26	67.71	66.25	64.31	69.79
Al_2O_3	19.09	18.89	18.43	18.38	18.32	17.94	18.73	18.50	18.23	18.57	19.48	19.35	18.18	17.62
FeOt	0.74	0.32	0.33	0.27	1.02	0.36	0.37	0.15	0.25	0.40	0.20	0.20	0.20	0.32
CaO	0.13	0.34	0.05	0.02	0.18	0.41	0.27	0.18	0.19	0.21	0.47	0.49	0.03	0.64
Na_2O	0.50	4.23	0.94	0.57	0.56	0.62	2.93	2.28	1.47	2.54	8.61	6.35	0.72	7.13
K_2O	15.77	10.25	15.09	16.09	15.56	15.80	11.89	13.08	14.28	13.07	4.80	7.05	15.57	5.48
BaO	0.44	0.10	0.65	0.08	0.03	0.23	0.10	0.31	0.10	0.37	0.07	0.06	0.23	0.16
sum	102.48	100.44	100.61	100.70	100.00	100.26	100.44	99.65	100.80	100.43	101.35	99.76	99.25	101.14
Si (a.p.f.u.)	2.965	2.996	2.999	2.998	2.964	2.994	3.014	3.003	3.030	2.975	2.964	2.981	2.997	3.103
Al	1.014	1.006	1.000	0.995	0.995	0.975	1.006	1.005	0.982	0.998	1.005	1.026	0.998	0.924
Fe	0.028	0.012	0.013	0.010	0.039	0.014	0.014	0.006	0.009	0.015	0.007	0.008	0.008	0.012
Ca	0.006	0.016	0.002	0.001	0.009	0.020	0.013	0.009	0.009	0.010	0.022	0.024	0.002	0.030
Na	0.044	0.371	0.084	0.051	0.050	0.055	0.259	0.204	0.131	0.224	0.731	0.554	0.065	0.615
K	0.906	0.591	0.887	0.943	0.915	0.930	0.691	0.769	0.833	0.760	0.268	0.405	0.925	0.311
Ba	0.008	0.002	0.012	0.002	0.001	0.004	0.002	0.006	0.002	0.007	0.001	0.001	0.004	0.003
Or	94.73	60.43	91.11	94.80	93.98	92.47	71.77	78.33	85.64	76.41	26.25	41.20	93.24	32.50
Ab	4.60	37.91	8.66	5.10	5.10	5.51	26.89	20.78	13.42	22.56	71.59	56.38	6.59	64.32
An	0.67	1.66	0.23	0.09	0.92	2.02	1.35	0.89	0.93	1.03	2.15	2.42	0.17	3.19

Table 5. Major and trace element analyses of dolerite dyke swarms of Hama Koussou tholeiites and CIPW normative compositions calculated according to a Fe_2O_3/FeO ratio of 0.15

Lava	Basalt		Basaltic trach	Trachyandesite		
Sample	**L1**	**M3**	**HB2**	**J6**	**J4**	**M5**
SiO_2 (wt. %)	46.49	46.87	51.58	55.97	55.98	56.02
TiO_2	2.70	2.59	2.96	1.73	1.69	1.74
Al_2O_3	16.23	16.62	14.55	16.29	16.41	16.27
Fe_2O_3	13.04	13.78	10.87	7.42	7.40	7.51
MnO	0.15	0.17	0.14	0.09	0.09	0.09
MgO	5.45	5.56	3.58	3.32	3.21	3.40
CaO	7.85	7.74	6.70	5.67	5.38	5.36
Na_2O	2.81	3.17	3.25	3.69	3.75	3.74
K_2O	2.13	1.29	2.82	3.43	3.70	3.52
P_2O5	0.41	0.38	0.70	0.51	0.52	0.53
LOI	2.4	1.5	2.26	1.4	1.4	1.4
sum	99.66	99.67	99.41	99.52	99.53	99.58
CIPW Norm						
Quartz	0.00	0.00	2.13	3.87	3.13	3.60
Orthoclase	12.59	7.62	16.67	20.27	21.87	20.80
Albite	23.78	26.82	27.47	31.22	31.73	31.65
Anorthite	25.38	27.31	16.80	17.75	17.02	17.21
Diopside	9.01	7.14	9.86	5.81	5.18	4.88
Hypersthene	1.37	5.36	14.15	12.79	12.86	13.55
Olivine	15.66	14.52	0.00	0.00	0.00	0.00
Magnetite	2.25	2.38	1.87	1.28	1.28	1.29
Ilmenite	5.13	4.92	5.61	3.29	3.21	3.30
Apatite	0.95	0.88	1.62	1.18	1.20	1.23
Rb (ppm)	110.1	24.5	74.34	80.6	86.4	85.1
Sr	640.7	607.8	748.6	843.5	854.7	817.5
Cs	3.3	1.8	2.868	2.6	2.3	2.7
Ba	505	443	918.8	1383	1419	1302
Be	<1	<1	1.987	5	<1	3
V	224	220	212	159	157	156
Cr	1.17	1.17	6.672	2.925	2.34	3.51
Co	41.0	49.3	30.62	21.7	20.7	21.7
Sc	20	19	16.59	11	11	11
Ni	34	44	14.43	27	29	31
Cu	18	28	27.11	29	26	31
Zn	117	121	144.3	87	83	92
Y	25.3	22.9	35.84	17.1	17.0	15.9
Zr	203.1	184.7	385.8	324.4	316.9	316.0
Nb	18.9	17.5	31.66	13.7	13.3	13.0
Hf	4.8	4.4	9.094	7.7	7.5	7.2
Ta	1.2	1.0	2.523	0.9	0.9	0.8
Th	1.9	1.8	4.913	12.5	12.9	12.3
U	0.5	0.3	1.106	1.5	1.6	1.4
La	25.3	21.8	46.92	58.7	61.1	57.9
Ce	54.1	48.7	102.2	115.1	117.0	114.6
Pr	6.87	6.17	13.27	12.75	12.82	12.66
Nd	28.9	26.6	55.7	46.7	47.7	46.1
Sm	6.34	5.74	11.77	8.48	7.92	7.96
Eu	2.24	1.92	3.307	2.13	2.12	2.10
Gd	6.18	5.77	9.614	6.13	5.99	6.19
Tb	0.96	0.89	1.34	0.76	0.73	0.76
Dy	5.03	4.47	7.34	3.63	3.56	3.55
Ho	1.03	0.93	1.357	0.62	0.63	0.60

Lava		Basalt	Basaltic trach	Trachyandesite		
Sample	**L1**	**M3**	**HB2**	**J6**	**J4**	**M5**
Er	2.88	2.47	3.229	1.54	1.58	1.58
Tm	0.36	0.36	0.422	0.21	0.21	0.20
Yb	2.33	2.28	2.656	1.24	1.18	1.34
Lu	0.33	0.33	0.371	0.18	0.19	0.19
Pb	5.0	2.6	8.9268	5.9	5.8	5.8
W	4.7	<0.5	0.815	0.6	0.7	0.9

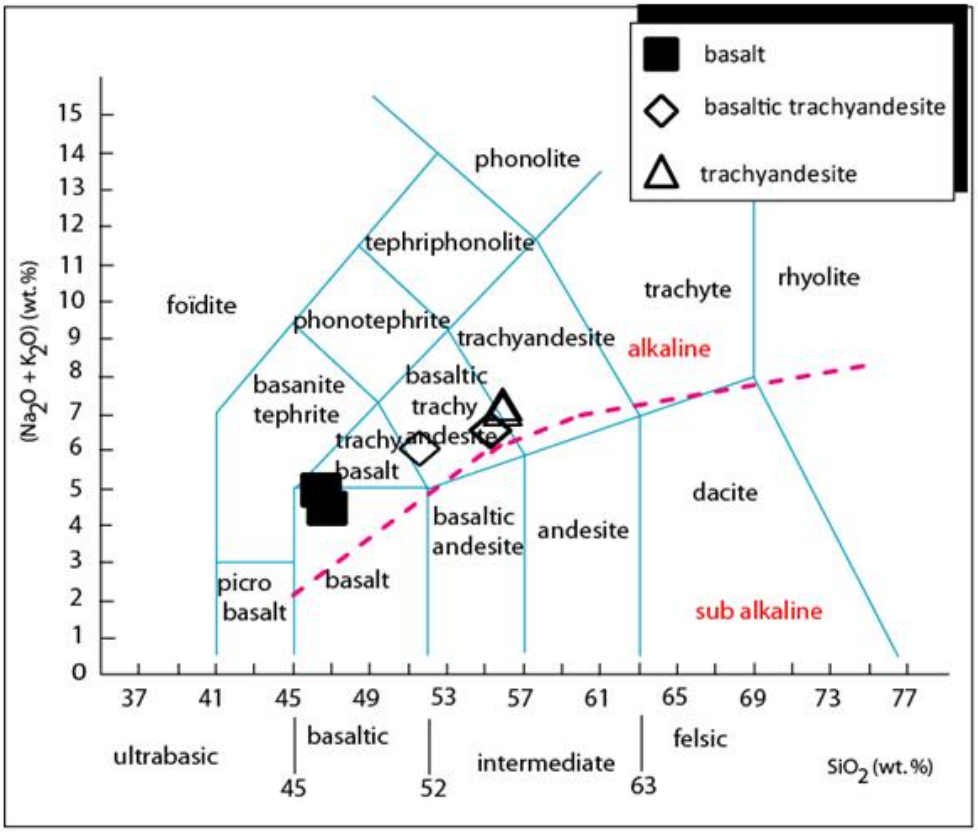

Fig. 7. Total alkali-silica diagram showing Hama Koussou basin dykes with root names (wt. % volatile-free recalculated compositions, after [13]). Demarcation dashed line between alkaline and subalkaline is after [15]

Normalized trace element patterns are presented in Fig. 9A. They show parallel trends with decreasing normalized values from incompatible to compatible elements. Specifically, dolerites of basalt composition exhibit negative anomalies in Rb, Nb, Ta, P and Ti and positive anomaly in K. Evolved dolerites show positive anomalies in Ba, K and Y and negative anomalies in Nb, Ta, P and Ti. In (Thn/Ybn) vs Mg# diagram (Figure not shown) of [19], dolerites of basalt composition fall within the spinel stability domain (Thn/Ybn<2). Th/Yb vs Nb/Yb diagram (Fig. 10) of [20] shows the location of Hama Koussou dolerite of basalt composition near E-MORB setting and the evolved dolerites lavas toward magma-crust interaction trend.

Normalized REE of Hama Koussou dolerites (Fig. 9B) show sloping patterns with LREE amounts reaching 90 times the mantle values in trachyandesite (only 40 times for basalt) whereas HREE amounts are relatively high in basalt. (Ce/Yb)n ratios are low for basalt (5.5 to 6) and high (22 to 26) in more evolved dolerites (with Th/Ta between 14 and 15). (La/Yb)n vary wildly (6.5-35.0) from basalt containing low (La/Yb)n value to evolved lavas characterized by high value of this ratio.

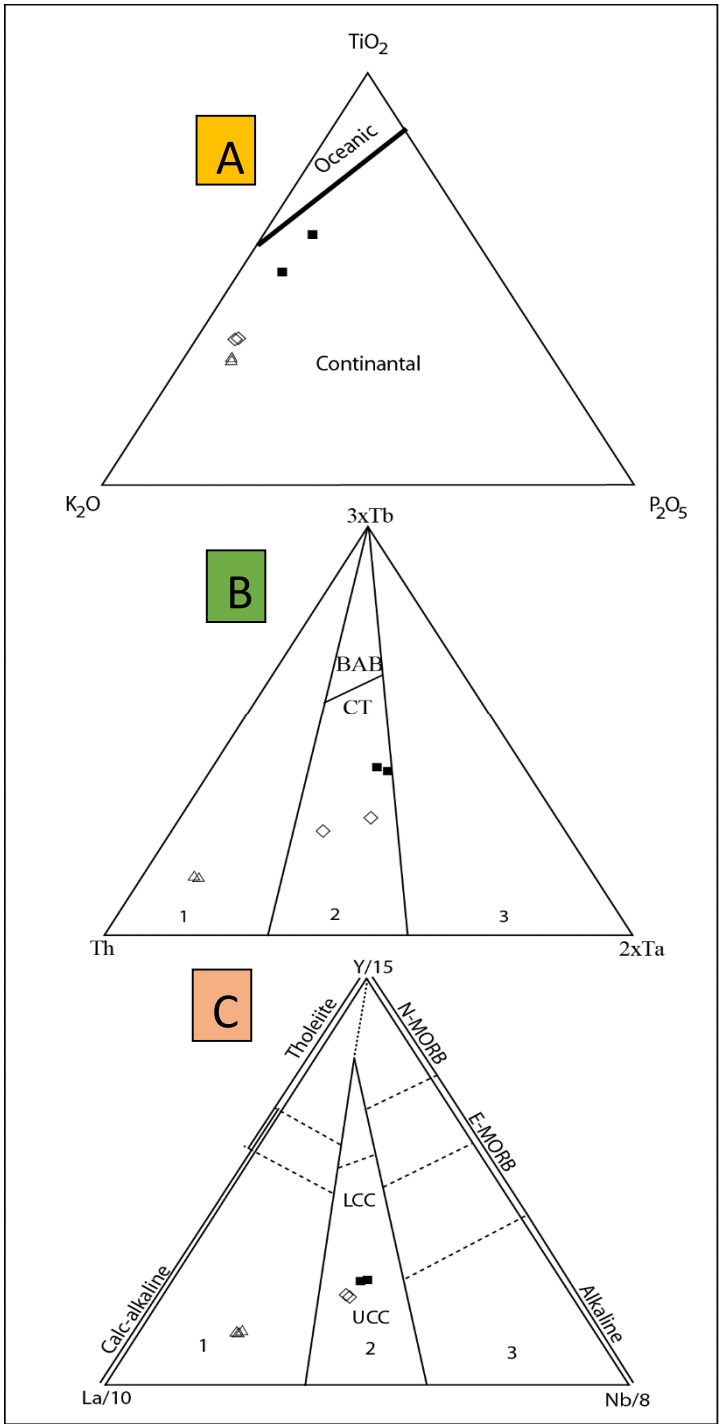

Fig. 8. Composition of Hama Koussou dolerites plotted in (A): TiO_2-K_2O-P_2O_5 after [18], (B): Tb-Th-Ta after [16], BAB: Back Arc Basin Basalt, CT: Continental Tholeiites; 1. Orogenic basalts, 2. Continental tholeiites and arc basin basalts and 3. Non orogenic basalts. (C): Y-La-Nb after [17], CC: Continental Crust (mean value), LCC: Lower Continental Crust, UCC: Upper Continental Crust; 1: Arc-related orogenic series, 2. Intermediate domain of continental tholeiites and 3. Anorogenic series of oceanic ridges and intraplate alkaline basalts. Same symbols as Fig. 6

5. DISCUSSION

Petrography, mineralogy and geochemical data of Hama Koussou half graben dolerite dyke swarm underscore the intrusive lavas of continental tholeiites composition (after [21,22,23]). The width of dolerite dykes of Hama Koussou (4 to 6 m) point out the "giant dykes" features [24] of studied lavas, typical of geological extensional setting. N05, N50 and N70 trending directions of Hama Koussou dolerite dyke swarms correspond to well-known pan African basement lineaments and faults [25,26] whose trends formed precursor rift directions for the development of West and Central African Rift System (CARS) during the Pan African crustal consolidation [3,5,27,28]. The Hama Koussou dolerites may thus be considered as the records of stress conditions just after Pan African consolidation feeding weak crustal cracks of the Pan African mobile zones prior to development of magmatic system relative to extensional setting at Late Jurassic-Early Cretaceous times [8] leading to the development of the West and Central African rift systems [3,5,8].

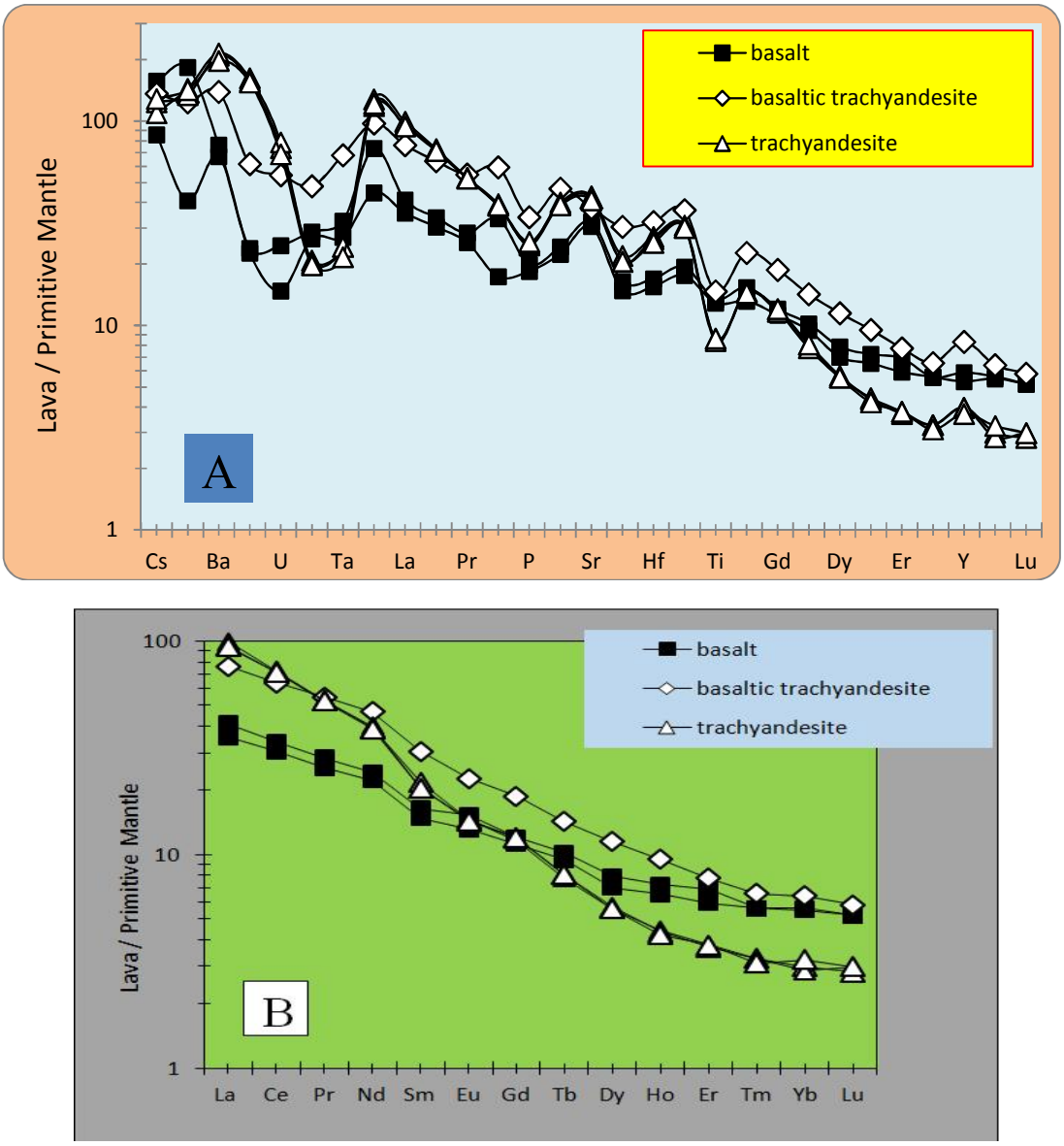

Fig. 9. Primitive mantle (after [29]) normalized incompatible trace element (A) and REE (B) of dolerites dykes from Hama Koussou basin

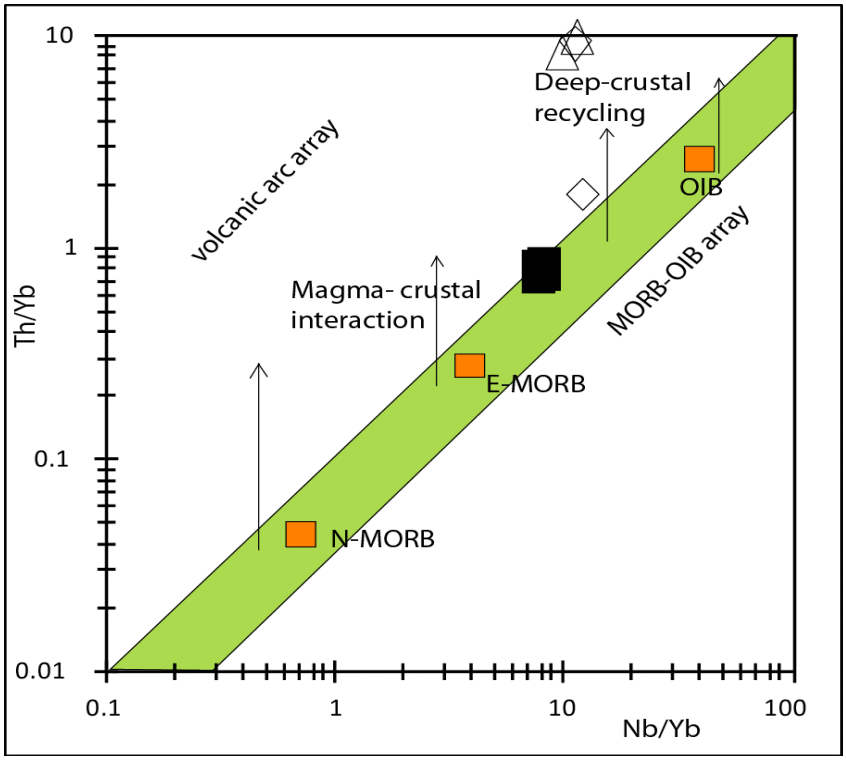

Fig. 10. Th/Yb vs Nb/Yb diagram after [20] of Hama Koussou dolerites. Same symbols as those shown in Fig. 9

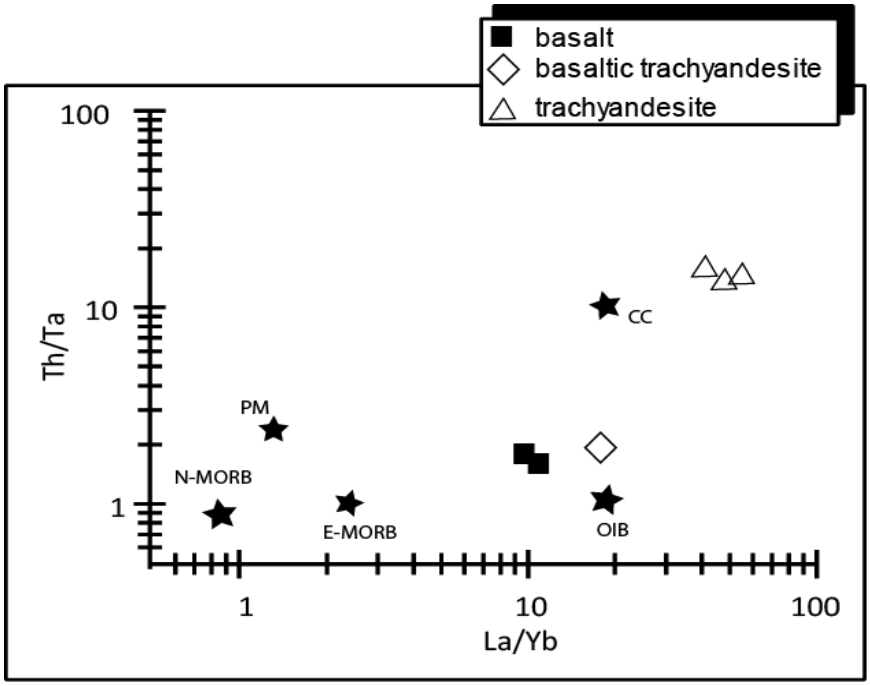

Fig. 11. Th/Ta vs La/Yb diagram of Hama Koussou dolerites (after [30]; OIB, E-MORB, N-MORB and PM (Parental Magma) from [3]; Continental Crust (CC) from [32]

Mineralogical compositions of Hama Koussou dolerites evolve from diopside to augite for clinopyroxene and labradorite to albite via andesine and oligoclase for plagioclase, and anorthoclase to sanidine for alkali feldspar. This evolutional composition is the result of fractional crystallization leading to magma differentiation coupled with crustal contamination as proposed by [33] probably trough assimilation or digestion processes of crustal rocks. Fluid circulation is suspected as attested by the alteration features of some mineral phases [34].

ICP-MS and ICP-AES geochemical analyses of Hama Koussou dolerites distinguish dolerites of basalt, basaltic trachyandesite and trachyandesite compositions among those lavas. At the sight of this composition, one may easily suggest a magma differentiation trough fractional crystallization process involving clinopyroxene, plagioclase, alkali feldspar and oxides crystallization trends of tholeiite lavas [34]. Dolerite of basalt composition exhibit olivine thloleiite saturated lavas features as suggest the results of norm calculation (see Table 5). It may have undergone an early compositional evolutions attested by it low Mg# (<67%). Ni, Cr and Co contents of this lava are also low and strongly argue for this hypothesis. Low (Ce/Yb)n ratios suggest an extensive partial melting rate. Using the empirical formulae of P (kbar) = 213.6-4.05 SiO_2 of [35], dolerites basalt may have been formed between 23.78 and 25.32 kbar. Accordingly, maximum depths of origin of Hama Koussou basalt are 60.5-55.5 km (considering the underlined crust of 23 km, [36]), if one uses a conversion factor of 33 km × GPa^{-1}, that is to say in the spinel stability field as suggested by the low Thn/Ybn ratios (<2). The mantle source of Hama Koussou dolerites may thus be the lithospheric mantle of E-MORB composition if one considers the location of dolerites basalt in Th/Yb vs Nb/Yb diagram (Fig. 10) of [20] and Th/Ta vs La/Yb diagram (Fig. 11, after 30] or relatively high contents of incompatible and LREE elements [37]. Geodynamic setting of studied lavas could be a post orogenic extensional domain after subduction or a field of post Pan African orogeny relaxation. Differentiated dolerites were formed near the surface, probably within the pan African cracks after crystallization of phenocrysts of clinopyroxene, plagioclase and others minerals. Magma processes other than fractional crystallization may have occurred during their petrogenesis. Contamination by crustal materials (Figs. 10 and 11) trough Assimilation and Fractional Crystallization (AFC) of differentiated dolerites is attested by high Sr, Ba and Nd contents of those lavas [38] and the involvement of fluid circulation is attested by occurrence of pyrite and chlorite secondary minerals and relatively high Mg# of dolerites more evolved than basalt [34].

6. CONCLUSION

Dolerite dyke swarms of Hama Koussou basin located North of the Yola branch of Benue trough in Cameroon are continental tholeiites. They are considered as fingerprints of post Pan African relaxation phase prior to Late Jurassic-Early Cretaceous extensional markers which have led the development of the West and Central African rift systems. The Hama Koussou continental tholeiites are the results of an extensive partial melting rate of E-MORB mantle source of spinel lherzolite composition, located at 55-65 km under the continental crust. Differentiation trough fractional crystallization process of tholeiite basalts and the involvement of crustal materials and hydrothermal processes have led to development of evolved Hama Koussou tholeiite lavas.

ACKNOWLEDGEMENTS

Authors warmly thank the “Agence Universitaire de la Francophonie (AUF)” for financial support for microprobe analyses. We are grateful to the University of Paris-Sud Orsay, France, for thin sections and to the blinds reviewers which remarks have greatly improved this manuscript.

COMPETING INTERESTS

Authors have declared that no competing interests exist.

REFERENCES

1. Maurin JC, Guiraud R. Relationships between tectonics and sedimentation in the Barremo-Aptian intra- continental basins of Northern Cameroon. In: CA Kogbe and J. Lang (Editors), African Continental Phanerozoic Sediments. Journal of African Earth Sciences. 1990;10(1/2):331-340.
2. Cratchley CR, Louis P, Ajakaiye DE. Geophysical and geological evidence for the Benue-Chad Basin Cretaceous rift valley system and its tectonic implications. Journal of African Earth Sciences. 1984; 2(2):141-150.

3. Genik GJ. Regional framework, structural and petroleum aspects of rift basins in Niger, Chad and the Central African Republic (C.A.R.). Tectonophysics.1992;213:169-185.
4. Fairhead JD. Mesozoic plate tectonic reconstructions of the central South Atlantic Ocean – The role of the West and Central African Rift system in Nigeria and Cameroon and its tectonic interpretation. Tectonophysics. 1988;143:141-159.
5. Binks RM, Fairhead JD. A plate tectonic setting for Mesozoic rifts of west and Central Africa. In: P.A. Ziegler (Editor), Geodynamics of Rifting, Volume II. Case History Studies on Rifts: North and South America and Africa. Tectonophysics. 1992;213:141-151.
6. Kröner, A., Stern, R.J. Pan-African Orogeny. Encyclopedia of Geology.2004;1:1-12.
7. Toteu, S.F., Penaye, J, Poudjom Djomani, Y. Geodynamic evolution of the Pan-African belt in Central Africa with special reference to Cameroon. Canadian Journal of Earth Sciences. 2004; 41(1):73-85.
8. Maurin JC, Guiraud R. Basement control in the development of the Early Cretaceous West and Central African Rift System. Tectonophysics. 1993;228:81-95.
9. Ntsama Atangana J. Magnétostratigraphie et sédimentologie des formations crétacées des bassins sédimentaires d'Hamakoussou et du Mayo Oulo-Léré au Nord-Cameroun (Fossé de la Bénoué). Thèse Terre solide et enveloppes superficielles, Université de Poitiers. 2013; 211.
10. Nkouandou OF, Ngounouno I, Déruelle B. Geochemistry of recent basaltic lavas from the north and east of Ngaoundéré zones (Cameroon, Adamawa Plateau, Central Africa): petrogenesis and the nature of the source. International Journal of Biological and Chemical Sciences. 2010;4:984-1003.
11. Pouchou JL, Pichoir F. Quantitative analysis of homogeneous or stratified microvolumes applying the model “PAP”. In: Heinriche, D.E. (ed) Electron Probe Quantification. Plenum Press, New York. 1991;31-75.
12. Morimoto N, Fabries J, Ferguson AK, Ginzburg IV, Ross M, Seifert FA, Zussman J, Aoki K, Gottardi G. Nomenclature of pyroxenes. Mineralogical Magazine. 1988;52:535-550.
13. Le Maitre, RW. Igneous Rocks: A classification and glossary of terms. Recommendations of the IUGS Sub-Commission on the Systematics of Igneous Rocks, 2nd edition. Cambridge University Press, Cambridge; 2002.
14. Carmichael ISE, Turner FJ, Verhoogen J. Igneous petrology. McGraw-Hill, New York; 1974.
15. Miyashiro A. Nature of alkalic volcanic rock series. Contributions to Mineralogy and Petrology. 1978;66:91-104.
16. Cabanis B, Thiéblemont D. La discrimination des tholéiites continentales et des basaltes arrière-arc. Proposition d’un nouveau diagramme Th-Tbx3-Tax2. Bulletin de la Société Géologique de France. 1988;8(6):927-935.
17. Cabanis B, Lecolle M. Le diagramme La/10-Y/15-Nb/8: Un outil pour la discrimination des séries volcaniques et la mise en évidence des processus de mélange et/ou de contamination crustale. Comptes Rendus de l’Académie des Sciences, Paris. 1989;309:2023-2029.
18. Pearce TH, Gorman BE, Birkett TC. The TiO_2–K_2O–P_2O_5 diagram: A method of discriminating between oceanic and non-oceanic basalts. Earth and Planetary Science Letters. 1975;24:419-426.
19. Wang K, Plank T, Walker JD, Smith EI. A mantle melting profile across the Basin and Range, SW USA. Journal of Geophysical Research. 2002;107:ECV5-1-ECV 5-21.
20. Pearce JA. Geochemical fingerprinting of oceanic basalts with applications to ophiolite classification and the search for Archean oceanic crust. Lithos. 2008;100:14-48.
21. Pearce JA, Cann JR. Tectonic setting of basic volcanic rocks determined using trace element analyses, Earth and Planetary Science Letters. 1973;19:290-300.
22. Campbell IH. The difference between oceanic and continental tholeiites: A fluid dynamic explanation. Contribution to Mineralogy and Petrology. 1985;91:37-43.
23. Holm PE. The geochemical fingerprints of different tectonomagmatic environments using hygromagmatophile element abundances of tholeiitic basalts and basaltic andesites. Chemical Geology. 1985;51:303-323.

24. Bryan SE, Ernst RE. Revised definition of large igneous provinces (LIPs). Earth Science Reviews. 2008;86:175-202.
25. Cornacchia M, Dars R. Un trait structural majeur du continent Africain. Les linéaments Centrafricains, du Cameroun au Golfe d'Aden. Bulletin de la Société Géologique de France. 1983;7(XXV):1:101-109.
26. Moreau C, Regnoult JM, Déruelle B, Robineau B. A new tectonic model for the Cameroon Line, Central Africa. Tectonophysics. 1987;139:317-334.
27. Guiraud R, Maurin JC. Early cretaceous rifts of western and Central Africa: An overview. In: P.A. Ziegler: (Editor). Geodynamics of Rifting, Volume II. Case 1 history studies on Rifts: North and South America, Africa-Arabia. Tectonophysics. 1992;213:153-368.
28. Benkhelil J, Mascle J, Guiraud M. Sedimentary and structural characteristics of the cretaceous along the Côte d'Ivoire-Ghana transform margin and in the Benue trough: A comparison. In Mascle, J., Lohmann, G.P., and Moullade, M. (Eds.). Proceedings of the Ocean Drilling Program, Scientific Results. 1998;159.
29. McDonough WF, Sun SS. The composition of the Earth. Chemical Geology. 1995;120:223-253.
30. Condie KC. Source of proterozoic mafic dykes swarms: Constraints from Th/Ta and La/Yb ratios. Precambrian Research. 1997;81:3-14.
31. Sun SS, McDonough WF. Chemical and isotopic systematics of oceanic basalts: Implications for the mantle composition and processes. In: Saunders, A. D., Norry, M. J. IEds.), Magmatism in the Ocean Basins. Geolgical Society London Publication. 1989;42:313-345.
32. Taylor SR, McLennan SM. The continental crust: It's composition and evolution. Blackwell, Oxford, UK. 1985;312.
33. Marzoli A, Chiaradia M, Jourdan F, Bussy F. Parental magmas and crustal contamination of continental tholeiitic basalts from the Central Atlantic magmatic province as revealed by mineral major and trace elements and Sr isotopes. Goldschmidt Conference Abstracts; 2006.
34. Cadman AC, Tarney J, Bridgwater D, Mengel F, Whitehouse MJ, Windley BF. The petrogenesis of the Kangâmiut dyke swarm, W. Greenland. Precambrian Research. 2001;105:183-203.
35. Scarrow JH, Cox KG. Basalts generated by decompressive adiabatic melting of a mantle plume: A case study from the Isle of Skye, NW Scotland, Journal of Petrology. 1995;36:3-22.
36. Poudjom Djomani YH, Diament M, Wilson M. Lithospheric structure across the Adamawa plateau (Cameroon) from gravity studies. Tectonophysics. 1997;273(3-4):317-328.
37. Dupuy C, Dostal J. Trace element geochemistry of some continental tholeiites. Earth and Planetary Science Letters. 1984;67:61-69.
38. Marsh JS. Geochemical constraints on coupled assimilation and fractional crystallization involving upper crustal compositions and continental tholeiitic magma. Earth and Planetary Science Letters. 1989;92:70-80.

Peer-review history:
The peer review history for this paper can be accessed here:
http://www.sdiarticle4.com/review-history/51594